Kondo resonance in the conductance of CoPc/Au(111) and TBrPP-Co/Cu(111)

J. M. Aguiar-Hualde,[1] G. Chiappe,[2] E. Louis,[2] E. V. Anda,[3] and J. Simonin[4]
[1]*Institut de Physique et de Chimie des Matériaux de Strasbourg (IPCMS), UMR 7504 CNRS-ULP, 23 rue du Loess, 67034 Strasbourg, France*
[2]*Departamento de Física Aplicada, Unidad Asociada del Consejo Superior de Investigaciones Científicas and Instituto Universitario de Materiales, Universidad de Alicante, San Vicente del Raspeig, Alicante 03690, Spain*
[3]*Departamento de Física, Pontificia Universidade Católica do Rio de Janeiro (PUC-Rio), 22452-970, Caixa Postal 38071 Rio de Janeiro, Brazil*
[4]*Centro Atómico de Bariloche and Instituto Balseiro, 8400 S.C. de Bariloche, Río Negro, Argentina*
(Received 26 June 2008; revised manuscript received 7 March 2009; published 10 April 2009)

Recent scanning tunnel microscopy experiments on transport through CoPc and TBrPP-Co molecules adsorbed on metallic surfaces have produced several interesting results: (i) a Kondo temperature much higher than that typically observed on undressed magnetic atoms adsorbed on metal surfaces, (ii) a Kondo resonance that shows up either as a Kondo peak (CoPc) or as a Fano dip (TBrPP-Co), (iii) in the CoPc/Au(111) system, the Kondo resonance shows up once the molecule has been distorted by cutting out eight peripheral hydrogens, and, (iv) in TBrPP-Co/Cu(111) the Kondo temperature depends strongly on the molecule conformation (either planar or saddle) and on the number of molecules around and close to the one through which the current flows. The aim of this work is to discuss these experiments within the framework of a simple model recently proposed by the authors which, capturing the main features of the inner structure of the molecule (four lobe orbitals plus a strongly correlated orbital), offers a physical interpretation for most of these observations.

DOI: 10.1103/PhysRevB.79.155415 PACS number(s): 73.63.Fg, 71.15.Mb

I. INTRODUCTION

One of the key issues in molecular electronics and spintronics is the reproducible control of electronic and spin currents. In recent years several possibilities of controlling the electronic conductance in systems showing a Kondo resonance[1,2] have been demonstrated.[3–8] Of particular relevance are the studies of the Kondo effect in transport through organic molecules containing a magnetic atom (*X*Pc and TBrPP-*X*, *X*=Co or Fe). It has been shown that the Kondo temperature may be varied by distorting the molecule[4] or by changing the number of neighboring molecules.[7] In addition, whether the Kondo effect manifests either as a Kondo peak or a Fano dip[9] may significantly depend on which molecule we are dealing with[4,6] and on the adsorption configuration of a given molecule.[8] Kondo temperatures in the range 130–600 K have been reported.[4,6–8]

The theoretical study of such systems needs to tackle two challenging problems: the complexity of the molecular electronic structure and the many-body effects derived from the presence of a magnetic atom. Taken into account exactly these two features is, at present, not feasible. Therefore, it is necessary to develop models that capturing the essential physics of the system simplify the description of the many-body interactions[10] and of the molecular electronic structure.[11] Recently, two of us have proposed a simple model[12] that allowed to analyze the experiments on CoPc/Au(111) (Ref. 12) and on TBrPP-Co/Cu(111) (Ref. 13) under the same framework. The model describes in a simple way the internal structure of the molecule. As argued below the minimal Hamiltonian that may account for the molecule inner structure of both CoPc and TBrPP-Co should include four one-orbital sites (describing the four molecular lobes, see below) plus a site with local correlations representing the magnetic atom (Co). Of course the model does also incorporate some additional one-orbital sites that represent the scanning tunnel microscope (STM) tip and the metallic surface on which the molecule is adsorbed. The aim of the present paper is to discuss in depth the main features of this model showing how, varying some of its key parameters *in accordance with the experimental information*, most of the experimental observations on those two systems find a natural, physical, and simple explanation. Besides the usefulness of presenting old material[12,13] from a unified point of view, a detailed analysis of the effects of molecule conformation on the Fano dip in TBrPP-CO/Cu(111) (Ref. 6) is presented; again the simple model of Ref. 12 seems to work adequately. Proposals for further experimental studies that may help in improving our understanding of these systems emerge from this analysis.

The rest of the paper is organized as follows. In Sec. II the experiments on which our analysis is focused are described in detail, highlighting the differences and similarities between the two molecules (Secs. II A and II B). The following Sec. II C is devoted to discuss the characteristics of the model Hamiltonian which are to a large extent based upon the experimental facts discussed in the previous subsections. The methods used to calculate the conductance are discussed in some detail in Sec. II D. Results are presented and discussed in Secs. III and IV. In Sec. III A the essential role played by the internal structure of the molecule in the transmission across it is highlighted both in what concerns the existence of the Kondo resonance as on whether the resonance manifests as a peak (CoPc) or as a dip (TBrPP-Co). Two additional subsections are devoted to an in-depth analysis of those two cases separately. Additional issues related to the system TBrPP-Co/Cu(111) are discussed in Sec. IV which in turn is subdivided in two subsections devoted to the effects of neighboring molecules, and the differences among

the two conformations that the molecule adopt when adsorbed on the metal surface. In the final Sec. V the main findings presented and discussed in this work are summarized.

II. EXPERIMENTAL OBSERVATIONS AND MODEL HAMILTONIAN

A. Summary of experimental observations

In this subsection we focus attention on the main features of the experiments on transport through CoPc adsorbed on Au(1,1,1),[4] and through TBrPP-Co adsorbed on Cu (1,1,1).[6,7] In the first experiment,[4] manipulation of the Kondo resonance was achieved by modifying the chemical surroundings of the Co atom through selective dehydrogenation of the molecule. In the initial state the topological conformation of the molecule consists of four well defined lobes, symmetrically disposed forming a square cross around the central Co atom and with no overlap between them. In this situation the system has no Kondo effect. Dehydrogenation is done by applying electrical pulses at the peripheral hydrogens of the molecule. In this way eight hydrogen atoms are cut away from the molecule. Concomitantly with this dehydrogenation process the molecule distorts in such a way that, once removed the eight hydrogens, the four lobes observed by STM merge into a single circular cloud surrounding the Co atom. When this occurs, the Co atom shifts up from the metal surface, while the lobes move down approaching the metal surface. In this situation the system shows Kondo effect with an abnormally high Kondo temperature ($T_K \sim 200$ K). The Kondo effect is observed as a zero bias wide peak in the curve of differential conductance versus bias voltage. Aiming to provide a sound explanation for the experimental observations, the authors carried out density-functional theory calculations.[4] They found that, while no magnetic moment was present in the undistorted molecule, the magnetic moment inherent to isolated Co was recovered upon dehydrogenation. From this result, however, the deeper conclusion one can derive is that, in the distorted molecule, the Kondo effect *may* show up.

The second series of experiments discussed here was carried out on TBrPP-Co/Cu (1,1,1). In its stable geometry (planar) the molecule does also show four lobes around the Co atom symmetrically disposed on a square. The authors of Ref. 7 highlighted their presence in the molecule (see Fig. 1 in Refs. 6 and 7) remarking that they provided higher current in the STM images. However, the lobes are not as cleanly defined as in the case of CoPc indicating that the overlap among them may be significantly higher. As regards to transport through this system, we note that the Kondo effect showed up as a Fano dip at zero bias in the curve of differential conductance versus bias voltage,[6,7] instead of the Kondo peak observed in the case of CoPc/Au(111).[4] The width of the dip gives a measure of the Kondo temperature of the system and, as shown in Ref. 7, it can be modified by changing the number of nearest-neighbor molecules around a given one. It was argued that a neighboring molecule locally removes the Cu(111) surface state,[14] thus reducing the density of states through which the current can flow and, hence, diminishing the Kondo temperature. In addition, the authors investigated the performance of a metastable conformation of the molecule, named saddle, as opposed to the planar stable conformation. In the saddle conformation the lobes ends lie at the corners of a rectangle, instead of the square observed in the planar conformation, and the highest STM current goes through two regions that are in between the two lobe pairs that are closer. In the saddle conformation the Co atom moves away from the metal surface. The main results derived from transport measurements are as follows:[6,7] (i) in both conformations a Fano dip is observed at the Fermi level characterized by a Kondo temperature that is higher in the planar conformation, and, (ii) the conductance through the planar conformation shows two peaks at bias voltages of approximately ± 0.7 V.

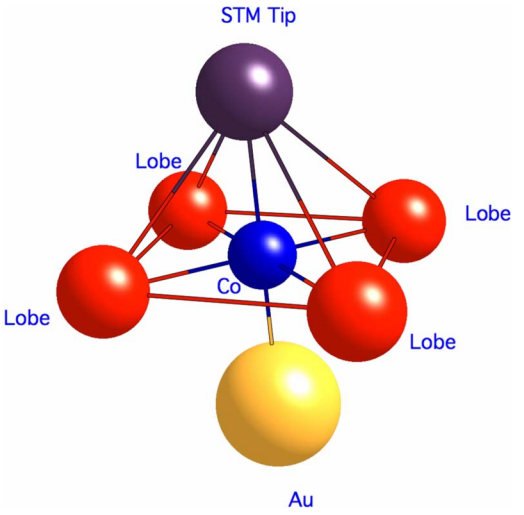

FIG. 1. (Color online) Cluster of atoms utilized to describe TBrPP-Co or CoPc adsorbed onto a metallic surface. The four sites on the square account for the four molecule lobes, while the atom at the center represents Co. The upper (lower) atom accounts for the apex of the tip of the STM microscope (metallic surface). To calculate the conductance a constant self-energy was attached to the top atom, the metallic atom, and the lobes (see text).

B. CoPc and TBrPP-Co: differences and similarities

These two molecules, although largely different, have two outstanding similarities: (i) both have the Co atom in the their geometric centers, and, (ii) their STM images show four clearly defined lobes.[4,6] Although the geometric conformation of both molecules is similar, the atomic neighborhood of Co in both cases is different. As a consequence the energy of the active d_{z^2} Co orbital is different in the two molecules. In the CoPc it has an energy around -0.15 eV, while it is much deeper in TBrPP-Co, around -0.7 eV. Due to this fact the coupling of the Co orbital with the tip and the metallic substrate orbitals is weaker in TBrPP-Co than in CoPc. As discussed below this has important consequences on the electronic conduction in these systems. Finally, as noted above, the fact that the four lobes appear to be less clearly defined in TBrPP-Co suggests that in this molecule the interaction among lobes is greater.

C. Model Hamiltonian

The model Hamiltonian used in this work (essentially an Anderson-Hubbard impurity Hamiltonian[15,16]) is based on the atomic arrangement depicted in Fig. 1 (Ref. 12): a central site (Co atom) with a single atomic orbital and a strong on-site repulsion, surrounded by four molecule lobes each one described by a single atomic orbital. Two additional sites, with one atomic orbital each, located above and below the Co atom are included to represent the apex of the STM tip and an atom on the metal surface, respectively. Then, the Hamiltonian takes the form

$$\hat{H} = \sum_{i\sigma} \epsilon_i c_{i\sigma}^{\dagger} c_{i\sigma} + \sum_{\langle ij\rangle;\sigma} t_{i,j} c_{i\sigma}^{\dagger} c_{j\sigma} + U n_{\mathrm{Co}\uparrow} n_{\mathrm{Co}\downarrow}, \qquad (1)$$

where $c_{i\sigma}^{\dagger}$ creates an electron at site i and spin σ and $n_{\mathrm{Co}\sigma}$ is the occupation operator acting on the Co orbital. $t_{i,j}$ is the hopping between atomic orbitals located on sites i and j (the symbol $\langle\ \rangle$ indicates that $i \neq j$). Each orbital has an energy ϵ_i and U is the local Coulomb repulsion on Co. The hopping matrix elements included here are as follows:[12] $t_{\mathrm{Co},t}$ (Co/STM tip), $t_{\mathrm{Co},m}$ (Co/metal surface), $t_{\mathrm{Co},l}$ (Co/molecule lobes) $t_{l,l}$ (interlobe hopping), $t_{l,m}$ (lobes/metal surface), and $t_{t,l}$ (tip/lobes). We assume that all orbitals, but that of Co, lie at the Fermi level, i.e., $\epsilon_i = 0$. As regards the d_{z^2} Co orbital we work in the symmetric case, namely, $\epsilon_{\mathrm{Co}} = -U/2$. We have checked that small variations in the orbital energies around those values do not qualitatively affect the main results. One of the leads is attached to the atom above Co and describes the STM tip, while the other lead (describing the metal surface) is attached to the atom below Co and to the lobes. Both leads are described by energy independent self-energies. A remark is in order: most of the calculations discussed here correspond to excessively large values of the couplings STM tip/lobes and STM tip/Co orbital (note that STM works in most experiments in the tunneling regime). This important issue is addressed in some detail in Sec. III B where it is argued that in most cases the effects of reducing those couplings is just a rescaling of the conductance.[17]

D. Conductance calculations

The differential conductance was calculated by means of a thoroughly tested finite U slave bosons (SB) approach[13,18–22] and by exact solutions of small clusters that are finally embedded with the leads through appropriate self-energies ["embedded cluster approximation" (ECA) see Ref. 23]. The SB approach is one of the few methods that allow to: (i) catch elusive many-body effects such as the Kondo resonance, and, (ii) work at finite bias voltages.[19,22] At low bias voltage, the Kondo effect dominates transport properties of the system. It is not the case at large bias voltage, where Coulomb blockade could be relevant and which is not properly captured by SB approach, but which, instead, is properly described by ECA. This will be discussed in more detail below. Since the SB method is essentially a single-particle approach, one obtains the current I through the molecule at bias voltage V by integrating the transmission probability:[24]

$$I(V) = \frac{e}{h} \int_{-\infty}^{\infty} T(E,V)[f(E-\mu_U) - f(E+\mu_L)]dE, \qquad (2)$$

where $f(E-\mu_{U,L})$ is the Fermi distribution for the left and right electrodes whose electrochemical potentials are denoted by μ_U and μ_L, respectively, and $\mu_U - \mu_L = eV$. The transmission coefficient $T(E,V)$ is given by

$$T(E,V) = \frac{2e^2}{h} \mathrm{Tr}[t^{\dagger} t]. \qquad (3)$$

In this expression, the matrix $t = \Gamma_U^{1/2} G^{(+)} \Gamma_L^{1/2}$, where $\Gamma_{U(L)} = i(\Sigma_{U(L)}^{(-)} - \Sigma_{U(L)}^{(+)})$, $\Sigma_{U(L)}^{(\pm)}$ being the self-energies of the upper (U) and lower (L) leads, STM tip and metallic surface, respectively. Superscripts (+) and (−) stand for retarded and advanced. The Green's function, in turn, is written as[24]

$$G^{(\pm)} = ([G_0^{(\pm)}]^{-1} - [\Sigma_U^{(\pm)} + \Sigma_L^{(\pm)}])^{-1}, \qquad (4)$$

where $G_0^{(\pm)}$ is the Green's function of the isolated cluster which depends on energy and bias voltage. The differential conductance was obtained by differentiating the numerical results for $I(V)$ with respect to the bias voltage. As regards to the second method (ECA) as all calculations correspond to $V=0$, the conductance is directly obtained from the transmission in Eq. (3). All calculations were done at zero temperature. Whenever not specified (see below) all out-of-equilibrium SB calculations were done assuming that the whole applied voltage dropped at the STM tip/molecule interface.

III. ORIGIN OF THE KONDO RESONANCE

This section is addressed to show the key role played by the molecule lobes in, (i) taking the system in or out the Kondo regime, and, (ii) determining whether the Kondo resonance would show up either as a Kondo peak or as a Fano dip. The results discussed hereafter clearly prove that the key parameters associated to those two effects are the lobe-lobe hopping and the lobe-tip hopping, respectively. General remarks are included in the first subsection, while the second and third are devoted to an in-depth analysis of the two systems here considered.

A. Role of the molecule lobes

The results depicted in Fig. 2 obtained by either ECA or SB methods (in Sec. III C it is shown that both give similar results over a rather wide energy range) clearly illustrate the relevance of the lobe-lobe coupling. We discuss first the results for zero lobe-tip hopping shown in the right panels of the figure. This case may describe the CoPc/Au(1111) system as, being the active d level of Co rather shallow, the direct hopping from the lobes to the tip might be substantially smaller than the Co-tip hopping. As remarked above, when the molecule is undistorted, the four lobes are clearly defined and one may safely assume that $t_{l,l}=0$. The conductance in this case shows no peak at the Fermi level, but rather two broad peaks below and above it. Actually, the broad feature peaked at around −0.15 eV might be that reported in Ref. 4 for the undistorted molecule. Note also that, when $t_{l,l}=0$, the

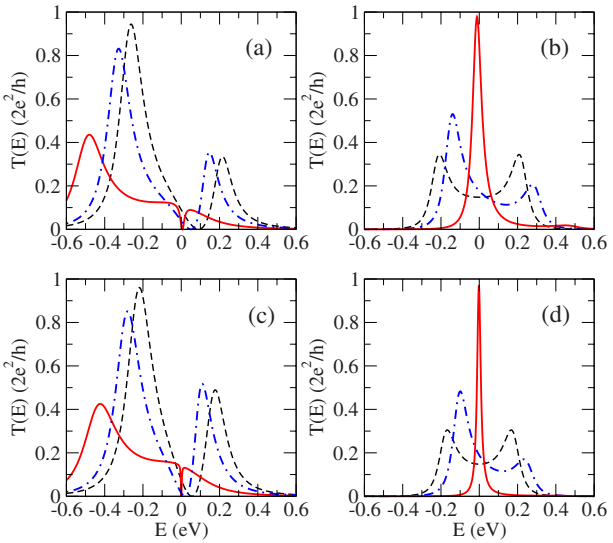

FIG. 2. (Color online) Transmission $T(E)$ (in units of the conductance quantum) versus the energy E (in eV) referred to the Fermi energy, calculated by means of the SB method (see text). The parameters used in the calculations are the following: $U=1.6$ eV (upper panels) and $U=2.3$ eV (lower panels), $t_{l,t}=0.06$ eV (left panels) and $t_{l,t}=0$ (right panels), $t_{l,l}=0.0$ eV (black broken line), $t_{l,l}=0.05$ eV (blue chain line), and $t_{l,l}=0.2$ eV (continuous red line). The rest of the model parameters are $t_{\mathrm{Co},m}=0.0$ eV, $t_{\mathrm{Co},l}=-0.14$ eV, $t_{\mathrm{Co},t}=0.08$ eV, $t_{l,m}=0.14$ eV, and $\rho_m=5$ eV^{-1}.

results are weakly dependent on U, revealing the noninteracting nature of the broad peaks around E_F. When the lobe-lobe interaction is finite (distorted molecule) the system enters into the Kondo regime and the conductance reaches the unit of conductance, while the Kondo resonance is narrowed as U is increased, indicating its many-body character. Although the actual value of the conductance depends on the ratio of Co-tip hopping to Co-lobe hopping, the physics is qualitatively similar (see Sec. IV for a more detailed discussion of this issue).

Results for finite lobe-tip interaction, $t_{l,t}=0.06$ eV, are shown in the left panels of Fig. 2. It is clear from this figure that the Kondo peak which characterized the previous case for finite lobe-lobe coupling has been replaced by a Fano dip. Now, when the lobe-lobe interaction is zero, the dip shows up as a rather broad minimum in the conductance appreciably shifted above the Fermi level. Switching on the lobe-lobe hopping fixes the conductance minimum at the Fermi level and substantially decreases its width. The conductance minimum that shows up for $t_{l,l}=0$ is a consequence of quantum interference between the different paths going across the molecule to the tip. This is essentially a one body effect, as its weak dependence on the value of U suggests. Instead for finite lobe-lobe hopping, the Fano dip shows a stronger dependence on U, becoming narrower as U is increased. This and the dip being fixed at the Fermi level are the hallmarks of the Kondo regime. Therefore, manipulating the lobe-lobe interaction, the position and the global shape of the Fano dip can be modified. It is interesting to note that, in the Kondo regime, while the Fano antiresonance coexists with a broad peak below the Fermi level, the Kondo peak in the case of

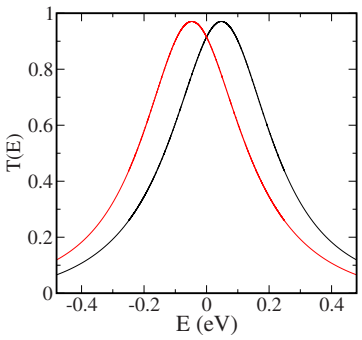

FIG. 3. (Color online) Transmission T (in units of the conductance quantum) versus energy E (in eV) for the Co uncoupled from the gold surface, i.e., $t_{\mathrm{Co},m}=0$. The rest of hoppings are as follows: $t_{\mathrm{Co},t}=0.5$ eV, $t_{\mathrm{Co},l}=1.25$ eV, $t_{l,m}=1$ eV, and, $t_{l,l}=2$ eV (red) $t_{l,l}=-2$ eV (black). The energy is referred to the Fermi energy.

CoPc does not (compare left and right panels in Fig. 2). This result is in line with experimental observations and is further discussed below.

The crucial role played by the lobe-lobe coupling is further illustrated in Figs. 3 and 4. In the case of CoPc, changing just the sign of the lobe/lobe hopping, which depends on the symmetry of the molecular orbitals, the maximum in the conductance, which lies just below the Fermi level ($t_{l,l}>0$) as observed in the experiments[4] is shifted upward; actually, the transmission is changed to $T(-E)$ when the lobe-lobe hopping changes sign (see Fig. 3). The transmission in the case of TBrPP-Co undergoes a more dramatic change when the sign of the lobe-lobe hopping is changed. Specifically, the Fano dip which shows up for $t_{l,l}>0$ is replaced by a line shape somewhat similar to that reported in Ref. 25, when the

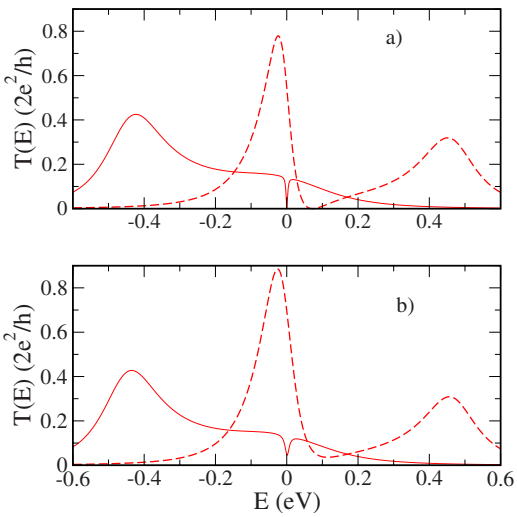

FIG. 4. (Color online) Transmission $T(E)$ (in units of the conductance quantum) versus the energy E (in eV) referred to the Fermi energy, calculated by means of the SB method (see text). The parameters varied in the calculations are $t_{l,l}=0.2$ eV (continuous red lines), $t_{l,l}=-0.2$ eV (broken red lines), and $t_{\mathrm{Co},m}=0.0$ eV (a) and $t_{\mathrm{Co},m}=0.08$ eV (b). The rest of the model parameters are $U=2.3$ eV, $t_{l,t}=0.06$ eV, $t_{\mathrm{Co},l}=-0.14$ eV, $t_{\mathrm{Co},t}=0.08$ eV, $t_{l,m}=0.14$ eV, and $\rho_m=5$ eV^{-1}.

sign of $t_{l,l}$ is changed (see Fig. 4). This effect is caused by the nontrivial internal structure of the molecule incorporated in our model, and has no relation with "external," probe-related, parameters such as tip-lobes and tip-Co hoppings. Changing the relative sign of $t_{l,l}$ and $t_{l,t}$ hopping modifies the level structure of the molecule and may change its net spin, driving the system in or out the Kondo regime (somehow as it occurs in CoPc when $t_{l,t}=0$ and the magnitude of $t_{l,l}$ is varied). On the other hand, these changes in the line shape are similar to results found for Co adsorbed on metal surfaces: (i) the oscillation of the tunneling DOS reported in Ref. 26 as the distance from the tip to the Co atom was varied, and, (ii) the changes in the conductance as the density of states of the metal substrate is varied.[25] Despite this similarity, most of the present results cannot be described within the simplest version of the Fano interference model, where the impurity has no internal structure.

These results illustrate the most essential feature of our work: the role of the molecular lobes is not only to participate in the screening of the spin at the Co atom, as the metallic surface does,[17] but also contributing to change dips into peaks[25,26] or even to drive the system in/out the Kondo regime. The net spin of the molecule, when adsorbed on a metallic surface that acts as a reservoir, is distributed over the whole molecule, not only on the Co atom, inducing a behavior that differs from that of the isolated Co atom.

B. CoPc/Au(111)

The results depicted in Fig. 5 are of particular value in identifying the origin of the emergence of the Kondo resonance upon distortion of the molecule.[4] As remarked above, the fact that the active d_{z^2} Co orbital is in this case closer to the Fermi level implies that the lobe-tip hopping is likely much smaller than the Co-tip hopping, and, thus, it can be neglected. We have chosen a set of parameters that differs substantially from that in the preceding subsection to illustrate the rather weak dependence of the main results on the model parameters. In order to see the influence of approaching the lobes to the metal surface, while the Co atom moves away from it in the distorted molecule, the results in the figure correspond to either the Co orbital [Fig. 5(a)] or the lobes [Fig. 5(b)] connected to the gold surface. In addition we assume either noninteracting lobes (green continuous line curves) or a finite hopping between lobes (red dashed line curves). The first case represents the undistorted molecule and the latter the distorted one. For comparison we also show the results for the standard Kondo effect in which the Co is decoupled from the molecule lobes (black curves). In line with the results of Fig. 2, the most appealing results are the following: when the molecule lobes do not interact no Kondo effect shows up, while when lobes interact among each other Kondo effect shows up with a critical temperature (which is proportional to the peak width) larger than in the case of an isolated Co atom.

We proceed now to discuss in some detail the origin of this remarkable result which is likely related to quantum interference.[2,11,12,27–31] To illustrate this assessment the phase difference between the direct path from the gold surface to the STM tip going through the Co atom, and the path that passes through the molecule lobes was calculated. This phase difference can be derived from the following element of the Green's function:

$$G^{(+)}(m,t) = g^{(+)}(m,t) + 4g^{(+)}(m,\mathrm{Co})\Sigma(\mathrm{Co},l)G^{(+)}(l,t), \quad (5)$$

where $\Sigma(\mathrm{Co},l)$ is a many-body self-energy that accounts for the lobes/Co coupling, and lower case "g" are the Green's functions in the case that lobes and Co are decoupled. The results shown in Fig. 5(c) are just the phase difference between the two terms in the right-hand side of Eq. (5). When there is no hopping between lobes, the phase difference is π indicating that the two terms may totally cancel each other, as actually occurs.

An alternative way to look at this issue is to calculate the local density of states (LDOS) on the Co atom that is obtained from the diagonal element of the Green's function. When there is a finite coupling between the molecule lobes, the diagonal element of the Green's function on the Co atom is

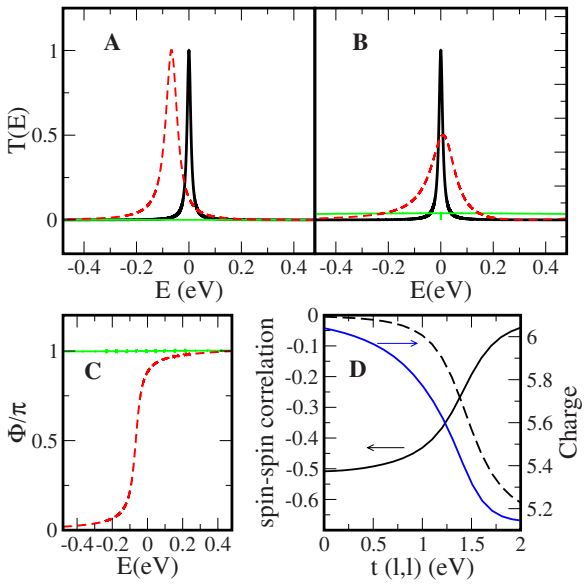

FIG. 5. (Color online) Transmission T (in units of the conductance quantum) versus the energy E (in eV) referred to the Fermi energy (A,B), phase difference Φ between the direct path from the gold surface to the STM tip going through the Co atom, and the path that passes through the molecule lobes (c) (see text) and charge into the molecule and spin-spin correlations between Co-lobes and Co-tip versus the lobe-lobe hopping (d). A: $t_{l,m}=0$, $t_{\mathrm{Co},t}=t_{\mathrm{Co},m}=0.25$ eV and $t_{\mathrm{Co},l}=1.25$ eV; $t_{l,l}=0$ (green continuous line), and $t_{l,l}=2$ eV (red dashed line). B: $t_{\mathrm{Co},m}=0$, $t_{\mathrm{Co},t}=0.25$ eV, $t_{l,m}=1$ eV, and, $t_{\mathrm{Co},l}=1.25$ eV; $t_{l,l}=0$ (green), and $t_{l,l}=2$ eV (red). The standard Kondo resonance, obtained with $t_{\mathrm{Co},l}=0$ and $t_{\mathrm{Co},t}=t_{\mathrm{Co},m}=0.25$ eV (black), is plotted in both (A and B). C: phase difference calculated for the parameters used in A. D: spin-spin correlation for Co/lobes (continuous line) and Co/STM tip (broken line) and total charge on the lobes plus Co (continuous blue line) versus $t_{l,l}$, for the parameters used in A. In all cases $U=8$ eV.

$$G^{(+)}(\mathrm{Co},\mathrm{Co}) = (\omega - \epsilon_l) g^{(+)}(\mathrm{Co},\mathrm{Co}) \times [(\omega - \epsilon_l) + \Sigma^2(\mathrm{Co},l) g^{(+)}(\mathrm{Co},\mathrm{Co})]^{-1}, \quad (6)$$

where $g^{(+)}(l,l')$ is the Green's function of the coupled lobes in the absence of Co/lobe coupling. When there is no coupling between the molecule lobes the latter Green's function takes the form

$$g^{(+)}(l,l') = \frac{1}{\omega - \epsilon_l} \delta_{l,l'}, \quad (7)$$

where ω is the energy referred to the Fermi energy, ϵ_l is the energy of the orbital lobes, and $\delta_{l,l'}$ is the Kronecker δ function;

$$G^{(+)}(\mathrm{Co},\mathrm{Co}) = (\omega - \epsilon_l) g^{(+)}(\mathrm{Co},\mathrm{Co}) \times [(\omega - \epsilon_l) + \Sigma^2(\mathrm{Co},l) g^{(+)}(\mathrm{Co},\mathrm{Co})]^{-1}. \quad (8)$$

It is readily seen that when the lobe orbitals lie at the Fermi energy (ϵ_l=0) the Green's function $G^{(+)}$(Co,Co) vanishes at that energy and, thus, the LDOS at the Co atom. A null density of states at the Fermi energy on the strongly correlated Co atom implies that no Kondo resonance should show up, in accordance with the phase analysis. Full cancellation of the two terms in the right-hand side of Eq. (5) is removed when the lobe orbitals do not lie exactly at E_F, a result that can be derived from Eq. (6). In this case no Kondo peak is present but the DOS at the Fermi level is different from 0. The conductance will be nonzero but no zero bias peak will be present. When coupling between lobes is switched on, the phase difference is no longer π [Fig. 5(c)] and the Kondo resonance shows up [Fig. 5(a)] (eventually, if lobe orbitals had nonzero energies, the peak would be situated at an energy close but different from zero). This results from the fact that switching on that coupling opens new paths for the electrons to go from the lobes to Co that contribute to the phase difference. Besides, the peak becomes significantly widened with respect to the standard Kondo effect (black curve in Fig. 5(a)) despite the fact that the molecule lobes are not connected to the gold surface. This is a consequence of the hybridization of Co and molecular lobe orbitals that increases the density of states on the Co atom leading to a Kondo temperature significantly larger than in the isolated Co atom.

Figure 5(d) shows the spin-spin correlation for Co lobes and Co tip (a similar result is obtained for Co-Au). Remarkably, switching on the lobe/lobe coupling shifts the antiferromagnetic correlation from the Co/lobes to the Co tip (in the undistorted molecule the spin on the Co orbital is screened by the spin on the lobes). In addition, six electrons are localized in the undistorted molecule (lobes plus Co). In this structure, when $t_{l,l}$=0, the atomic level of Co pushes down the four noninteracting lobe levels becoming the molecule charged with six particles due to its coupling with the leads. This indicates that when $t_{l,l}$ is zero the net spin in Co is screened by the lobes, occupied with five particles, preventing its Kondo coupling to the leads. The molecule charge is reduced down to five when the lobe/lobe coupling is switched on [see Fig. 5(d)], because its effect is to push up some of lobes levels. In this case the lobes, occupied with four particles, cannot screen the spin at the Co atom, which is now Kondo coupled to the leads. These results are consistent with the existence (absence) of a magnetic moment on the distorted (undistorted) molecule derived from the *ab initio* calculations reported in Ref. 4. The net spin is distributed over all the molecules. A similar result is obtained if a three lobe, instead of four, configuration is considered, indicating that the results do not depend on the number of electrons in the cluster. We believe that the mechanism hereby put forward for switching on and off the Kondo resonance may apply to a variety of situations.

Cutting out the bond between Co and the gold surface, and switching on those from lobes to gold, does not qualitatively change these results. Again, as shown in Fig. 5(b), in the absence of lobe-lobe coupling, no Kondo effect shows up. We note that even though the lobes-Au surface hopping in Fig. 5(b) is much higher than the Co-Au surface hopping used to obtain the results of Fig. 5(a), the width of the resonance is similar, albeit the peak height is considerably smaller (compare the red curves in those two figures). These results suggest that providing more ways to hybridize the atomic orbitals on the magnetic molecule to the continuum states (as may be in principle occur due to coupling of lobes to the gold surface) may not always be beneficial as far as the Kondo effect is concerned. It is finally noted that, as opposed to the results shown in Fig. 2, those depicted in Fig. 5 do not show two peaks close and around the Fermi level. This is probably due to the much larger relative value of the Co-lobe hopping taken to obtain the latter results.

C. TBrPP-Co/Cu(111)

As remarked above, one of the most interesting aspects of these molecules is that while in the case of CoPc a Kondo peak was observed, in the experiments on TBrPP-Co the conductance showed a Fano dip,[9] as in isolated Co atoms adsorbed on metal surfaces.[17,26,32,33] One of the main goals of our simplified model is to describe both systems in different parameter regions, giving a clear insight of the physics involved in each case. In this subsection we present results that were obtained using ECA and SB methods mainly addressed to further illustrate the origin of the Kondo effect in these systems.

As argued above, the fact that the active d_{z^2} Co orbital is much deeper in TBrPP-Co implies that its coupling to the STM tip orbital is substantially smaller than in CoPc. As a consequence, the coupling lobe-tip may become comparable to the coupling Co tip and can no longer be neglected as done in the case of CoPc. The consequences of this competition are further illustrated in Fig. 6. As shown in the figure, that competition is actually responsible for the transition from Kondo peak to Fano dip at zero bias. In order to make more apparent the crossover and compare with the analysis of Ref. 12, we took $t_{\mathrm{Co},m}$=0 (more realistic results are obtained taking a finite $t_{\mathrm{Co},m}$, see Sec. IV). To further illustrate this point we have calculated the nondiagonal elements of the density matrix using the standard expression

$$P(i,j) = \frac{1}{2\pi} \int_{-\infty}^{\infty} G^{<}(i,j;E) dE, \quad (9)$$

where $G^{<}(i,j;E)$ is the lesser Green's function of the whole system. The results shown in Fig. 6(c) indicate that $P(\mathrm{Co},t)$

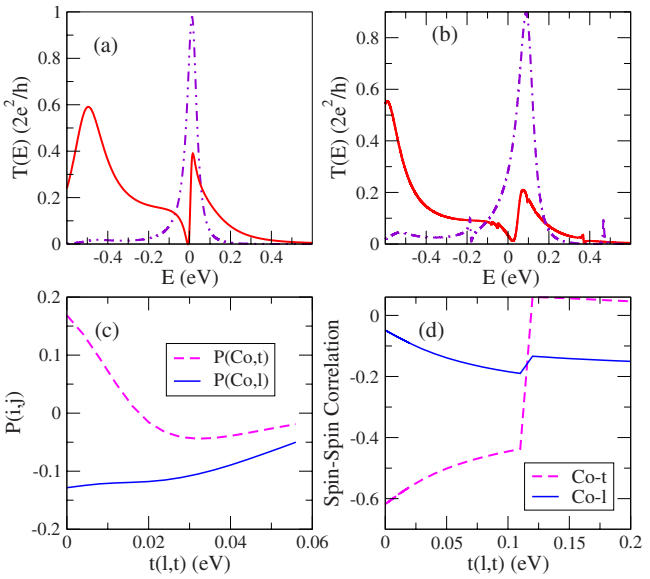

FIG. 6. (Color online) Upper panels: transmission $T(E)$ (in units of the conductance quantum) versus the energy E (in eV) referred to the Fermi energy, calculated by means of the SB (a) and the ECA (b) methods (see text). Results for $t_{l,t}=0$ (violet chain line) $t_{l,t}=0.08$ eV (continuous red line) are shown. (c) Nondiagonal elements of the density matrix versus $t_{l,t}$ as calculated by means of the SB approach. (d) Spin-spin correlation versus $t_{l,t}$ calculated by means of the ECA method. The rest of the parameters used in the calculations are $t_{\mathrm{Co},t}=0.08$ eV, $t_{\mathrm{Co},l}=-0.14$ eV, $t_{\mathrm{Co},m}=0$, $t_{l,l}=-0.2$ eV, $t_{l,m}=0.14$ eV, $U=1.6$ eV, and $\rho_m=5$ eV^{-1}.

is strongly reduced and tends to zero as the lobe-tip hopping becomes $t_{l,t}>t_{\mathrm{Co},t}$, triggering the crossover from a Kondo peak to a Fano dip. Therefore, the current flowing from Co to the tip reduces significantly, because the direct processes from Co to tip are suppressed. There is also a small reduction in $P(\mathrm{Co},l)$, that, however, remains significantly greater (in absolute value) than $P(\mathrm{Co},t)$ for $t_{l,t}>t_{\mathrm{Co},t}$. Consequently, a destructive interference among the electrons going directly from the tip to the metal through the lobes and those performing the same trajectory but visiting the Co atom, is induced, the last path being possible due to the Kondo resonance located at the Co atom. The effect is somewhat similar to that occurring in a correlation impurity side connected to a linear chain.

The results for the spin-spin correlation calculated with the ECA method shown in Fig. 6(d) clearly indicate that the strong antiferromagnetic correlation between Co and the tip, characteristic of the Kondo regime for $t_{\mathrm{Co},t}>t_{t,l}$ (Ref. 12), is destroyed as $t_{t,l}$ increases. In this case the Kondo regime is driven by the Co-lobe correlation that remains always antiferromagnetic. It should be noted that the spin-spin correlation changes abruptly because it corresponds to the isolated cluster which is exactly diagonalized when the ECA method is used. Results obtained by means of either SB or ECA methods [Figs. 6(a) and 6(b)] only differ at a quantitative level even away from the Fermi energy where, presumably, the SB method may not to be a good approximation. This indicates that at large energies, the relevant features of the transmission are well described by molecular levels associated to the noninteracting lobes rather than to the strongly correlated Co atom. The noticeable technical differences between the two approaches make this agreement particularly relevant. On the other hand, once confirmed that SB is reliable also at energies away from the Fermi level, this approach can be used for a simple implementation of out-of-equilibrium Keldysh formalism.[24] Thus, the results discussed in Sec. IV were all obtained with that method. In the case of the Fano dip, we note the presence of a broad peak at around −0.5 eV. This peak almost coincides with that observed experimentally at −0.7 eV that was ascribed to the d_{z^2} orbital, the one probably responsible for the strong correlation effects discussed here. However, such broad peak seems not to come from a pure Co level, as it is weakly connected to the leads. As just mentioned, we believe its origin to be associated to the noninteracting lobe orbitals. It should be noted that the latter peak shows up below E_F whenever both $t_{l,l}$ and $t_{\mathrm{Co},l}$ are negative. If they are assumed to be positive the results change to $T(-E)$ and if only one of them is negative the transmission is modified resembling less the experimental observations (a wider dip and a narrower peak below E_F, see above).

IV. FURTHER ANALYSIS OF THE TBrPP-Co/Cu(111) SYSTEM

A. Effects of neighboring molecules

In this subsection we analyze the effects of the density of states at the substrate surface on the Fano dip.[6] As suggested by the authors of Ref. 6, and already remarked above, molecules around a given one remove the Cu(111) surface state, thus reducing the local density of states ρ_m available for charge flow. Then, the larger the number of nearest neighbors nn the smaller ρ_m. The Kondo temperature may also depend on ρ_m in a way difficult to anticipate in such complex system. The effects of varying ρ_m on the Fano dip are illustrated in Fig. 7. In these calculations we have taken a value of $t_{\mathrm{Co},m}$ similar to that of $t_{\mathrm{Co},t}$ as it seems more realistic. Results for the transmission versus energy are shown in the upper panel, whereas the differential conductance versus bias voltage is shown in the lower panel. The latter was calculated by implementing Keldysh formalism into the SB approach.[19] It is noted that the two results are remarkably similar, as expected whenever the bias voltage is not very large.[34] At large voltages, peaks could be shifted, but qualitatively good agreement is also found. This supports the validity of the comparison of the transmission $T(E)$ with the experimental results. As shown in Fig. 7, increasing ρ_m widens the Fano antiresonance, and thus increases the Kondo temperature, as reported in Ref. 6. A rather different effect that is observed in Fig. 4 is the shifting of the dip peak to higher voltages. This shift was also observed in Ref. 6, although, unfortunately, a well defined tendency was not reported. We also note changes in the shape of the dip (particularly in the relative height of the left and right shoulders) also observed in the experimental study of Ref. 6. It should be noted that the values chosen for the couplings of the tip with Co and the lobes are surely too large; however, the shape of the curves remains unchanged if both are equally rescaled[17] [see dotted

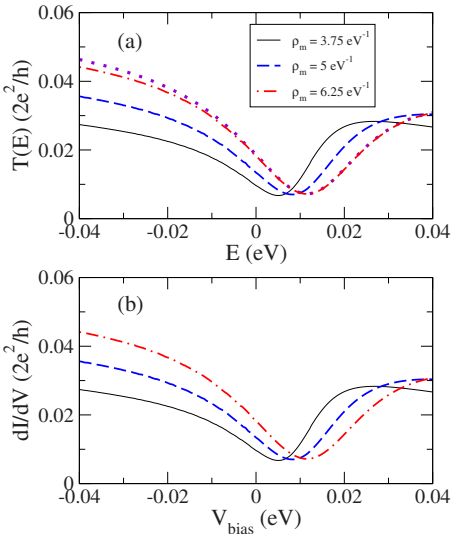

FIG. 7. (Color online) Transmission $T(E)$ (a) and differential conductance dI/dV (b) in units of the conductance quantum, versus either the energy E referred to the Fermi energy or the bias potential V_{bias} (in eV) as calculated by means of the SB method. Results for three values of the metal density of states ρ_m are shown. The rest of the model parameters are $t_{\text{Co},m}=0.04$ eV, $t_{\text{Co},l}=-0.14$ eV, $t_{\text{Co},t}=0.04$ eV, $t_{l,l}=-0.2$ eV, $t_{l,m}=0.14$ eV, $t_{l,t}=0.03$ eV, and $U=1.6$ eV. The dotted line in (a) depicts transmission results obtained with $\rho_m=6.25\ \text{eV}^{-1}$, $t_{l,t}=0.006$ eV, and $t_{\text{Co},t}=0.008$ eV (the rest of the model parameters as above), amplified by a factor of 675.

line in Fig. 7(a)]. Such large values were taken to reduce numerical errors due to the low values of the current.

B. Effects of molecule conformation: Planar versus saddle conformations

In order to analyze the differences between the conductance through either the saddle or the planar conformations reported in Ref. 6 and summarized above, we choose actual numerical values of the parameters to reproduce the main features seen in the conductance curve for the planar conformation (see Ref. 13 for details). Then, we investigate the effects of molecule conformation, *leaving up to some extent free a single parameter*: the coupling between the four molecule lobes. In particular, while the lobe/lobe hopping for the planar conformation was taken to be $t_{l,l}=0.2$ eV, as in Ref. 13, this value was rescaled for the saddle conformation in accordance with the changes in the lobe-lobe distance d reported in Ref. 6 and assuming that the lobe orbitals were p-like, that is, scaling hopping as d^{-3}, see Ref. 35 (scaling with a smaller power reduces the effects discussed here). The constant self-energy attached to the STM tip, the metal site below Co and the lobes was $\Sigma_{U(L)}^{(\pm)}=\mp 0.2i$ eV (the only role played by this parameter is to control the peaks widths in the conductance and the density of states).

An important issue is the way the applied bias voltage drops at the STM tip/molecule and at the molecule/metal surface contacts, a question whose answer would require a full *ab initio* calculation. Up to now we have assumed the molecule (Co atom plus four lobes) to be equipotential and

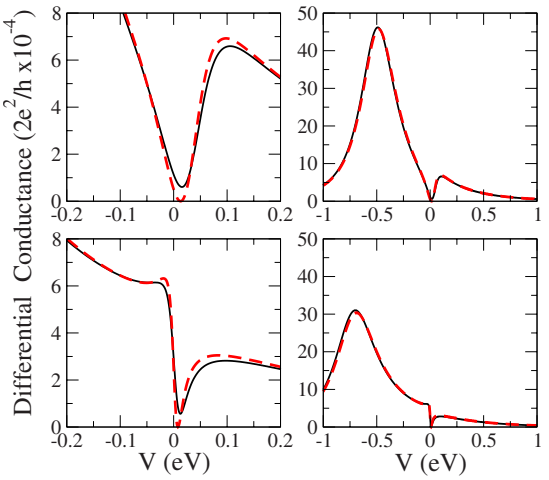

FIG. 8. (Color online) Differential conductance versus bias voltage V (in eV) at small (left panels) and large (right panels) voltage scales. The potential was assumed to drop entirely at the tip/molecule contact. Results for $t_{\text{Co},m}=0$ (red broken lines) and $t_{\text{Co},m}=0.2$ eV (black continuous lines) are shown. Upper panels: planar configuration (lobe-lobe hopping $t_{l,l}=0.2$ eV). Lower panels: saddle configuration (lobe-lobe hopping $t_{l,l}=0.56$ eV and 0.13 eV, see text). The rest of the model parameters are $t_{\text{Co},t}=t_{l,t}=-0.008$ eV, $t_{\text{Co},l}=0.16$ eV, and $U=1.6$ eV.

the whole voltage drop to occur at the STM tip/molecule contact. Here we keep the assumption of an equipotential molecule and explore three cases: (i) the whole drop at the STM tip/molecule contact, (ii) one fourth of the drop at the molecule/metal surface, and (iii) half drop at each contact. We first discuss the results corresponding to case (i) mainly for two reasons: (a) apparently this is the assumption most consistent with a STM tip weakly coupled to the molecule, and, (b) it gives a conductance versus voltage proportional to the transmission versus energy at zero bias voltage.

Figure 8 shows the conductance versus bias voltage for the molecule in the planar and saddle configurations. In order to highlight the structure around the Fermi level, curves are depicted over small and large voltage scales. Besides, results for two values of the Co/metal hopping are reported. We first note that the Fano dip at E_F narrows when the molecule is distorted. As shown in Ref. 6 the distortion occurs in such way that the relative increase in the two noncontiguous distances is smaller than the relative lowering of the other two. This means that, on average, lobe-lobe hopping has been increased. Therefore, the levels of the four interacting lobes become more separated after distortion, diminishing their contribution to the density of states at the Fermi energy. As a consequence, the width of the Fano dip decreases. Note that, had the distortion been the opposite (a relative lobe-lobe distance increase larger than the relative decrease) the Fano dip had widened. We have verified this result, which is one of the predictive conclusions of our model.

Another relevant observation derived from Fig. 8 concerns the role played by the coupling between Co and the metal surface: the results indicate clearly that it is not an important parameter of the model. The large conductance peak at around −0.5 eV corresponds to conduction through hybridized Co-lobes orbitals. It is noticeably decreased and

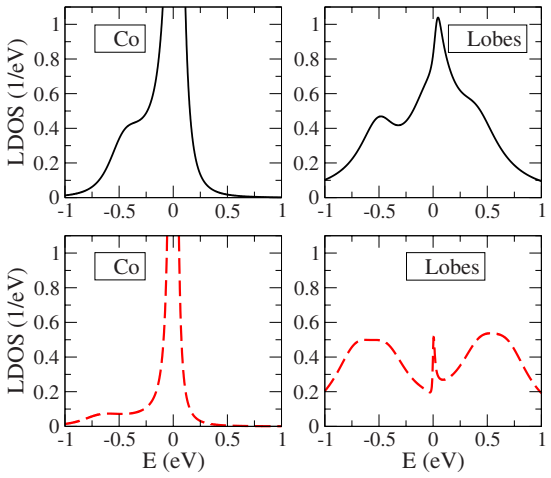

FIG. 9. (Color online) LDOS versus energy at Co (left panels) and lobes (right panels) orbitals. Upper panels: planar configuration (lobe-lobe hopping $t_{l,l}$=−0.2 eV). Lower panels: saddle configuration (lobe-lobe hoppings −0.56 eV and −0.13 eV, see text). The rest of the parameters are $t_{\mathrm{Co},m}$=0.04, $t_{\mathrm{Co},t}$=$t_{l,t}$=−0.008 eV, $t_{\mathrm{Co},l}$= −0.16 eV, and U=1.6 eV.

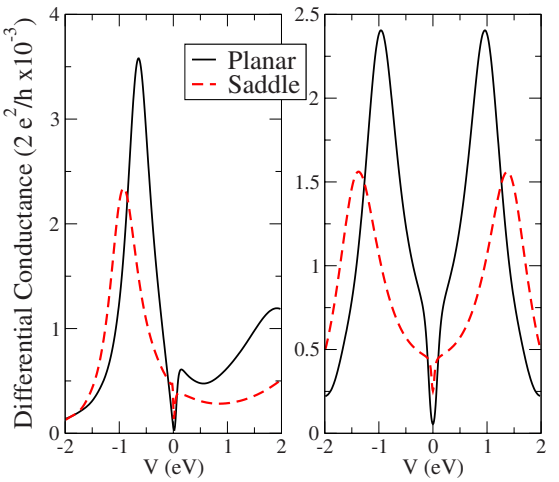

FIG. 10. (Color online) Differential conductance versus bias voltage V (in eV) for the planar (black continuous lines) and saddle (red broken lines) configurations. Left panel: the bias voltage drops 75% at the STM tip/molecule junction and 25% at the metal/molecule junction. Right panel: the bias voltage drops equally at the STM tip/molecule and metal/molecule contacts. In the planar configuration all lobe-lobe hoppings are $t_{l,l}$=0.2 eV, while in the saddle the two hoppings are 0.56 eV and 0.13 eV (see text) The rest of the parameters are $t_{\mathrm{Co},m}$=0.04, $t_{\mathrm{Co},t}$=$t_{l,t}$=−0.008 eV, $t_{\mathrm{Co},l}$ =0.16 eV, and U=1.6 eV.

shifted to lower energies when the molecule is distorted, no matter the actual value of the Co/metal hopping. Apparently, Co is tightly bound to the molecular lobes, which in turn are always bound to the metal surface (this is so even when the link between Co and metal surface is weakened). Therefore, shifting and depleting this peak in the conductance strongly depends on the inner structure of the molecule, and only slightly on the direct coupling between Co and metal surface.

This behavior is reflected also in the LDOS at Co and at the lobes (see Fig. 9). The four levels associated to the lobes when they are not coupled to the Co orbital are (we write only the sign of the weight of each state on each lobe): a fully symmetric level (FS)(+,+,+,+) with energy $2*t_{l,l}$, two antisymmetric levels (AS)(+,0,−,0) and (0,+,0,−) with energy 0 and a fully antisymmetric level (FAS)(+,−, +,−) with energy $-2*t_{l,l}$. Only the FS wave function is hybridized with Co orbital at $-U/2$ (see LDOS on Co at the left panels in Fig. 9) and contributes to the conductance. It is thus the origin of the broad peak around −0.5 eV in the differential conductance for the planar configuration. In the distorted molecule this peak shifts down and becomes wider, as can be seen in the lower panels of Fig. 9. This is so, because the mean lobe-lobe distance is reduced upon distortion, increasing the mean lobe-lobe hopping probability and reducing the DOS at the Fermi level. Note also that the Kondo peak at Co becomes narrower as the molecule is distorted. In addition, the symmetry of levels associated to lobes changes in such a way that their coupling to tip and Co is reduced. Consequently, the peak in the transmission curve is also reduced. An inverse distortion of the molecule (i.e., decreasing the mean value of the lobe-lobe hoppings) would have had the opposite effect, namely, shifting up the broad peak below the Fermi level and widening the Kondo resonance.

The above results differ from the experiments in that only the peak at −0.5 eV shows up (see Fig. 8). If our analysis is correct, the symmetry in the experimental results (peaks at ±0.5 eV) may indicate a more symmetric distribution of the voltage drop. Thus, as we do not know how the actual drop is (it would require a full *ab initio* calculation) we hereby report and discuss results for other potential drops and in particular for the symmetric one. Results obtained in the latter case are shown in the right panel of Fig. 10. A two-peak structure, similar to that observed in Ref. 6, results. This structure would be a consequence of the symmetric drop of the bias potential along the metal-molecule and molecule-tip junctions. These broad peaks are shifted down and up for the saddle configuration. Note that, although qualitatively similar to the results shown above, the effect of the molecular distortion is amplified when the bias voltage drops symmetrically (compare shiftings in Fig. 10 right panel with right upper and lower panels in Fig. 8). Finally, Fig. 10 shows results for the differential conductance when the voltage drops 75% at the tip/molecule and 25% at the metal/molecule contacts, to further illustrate the strong dependence of the results on the voltage distribution.

V. CONCLUDING REMARKS

Summarizing, a simple model has allowed us to account for the main features of the Kondo regime observed either as a Fano dip in TBrPP-Co/Cu(111) or as a Kondo peak in CoPc/Au(111). They are mostly consequence of the internal structure of the molecules which is incorporated into our model in a simplified way. In the case of CoPc/Au(111) we have been showed[12] that (i) quantum interference between STM tip/Co/lobes/metal surface and STM tip/Co/metal surface paths controls the entrance into the Kondo regime, and, (ii) hybridization of the Co atomic orbital with the molecular lobes increases the DOS on the Co atom, thus leading to a

Kondo temperature significantly larger than in the case of isolated Co. Our results are compatible with those obtained in Ref. 4 by means of *ab initio* calculations, particularly in what concerns the introduction of a net spin in the molecule that dehydrogenation produces. TBrPP-Co/Cu(111) results to be more complicated: the plausible higher value of the STM tip/lobes hopping (in relation to the STM tip/Co hopping), due to a different atomic environment of Co in this molecule, opens an additional path that increases the number of agents playing a role in quantum interference. However, the role of the lobes is crucial in both cases. We showed that changing the sign of the lobe/lobe hopping it is possible to change a Fano dip into a Kondo resonance, even when Co/tip and lobes/tip hoppings are of the same order of magnitude. The sign and magnitude of these parameters are determined by the electronic structure of the molecule, therefore allowing to simulate different kinds of molecules and behaviors within the same framework. It is worth pointing out that these effects are a consequence of the internal structure of the molecule incorporated in our simple model and could never be accounted for by the simplest version of the model used to discuss Fano interference.

The model not only allows to discuss the physics around the Fermi level in the Kondo regime, but also accounts for features in the experimental conductance below and above the Fermi level that coexist with the Fano dip, or does not exist when the transmission shows a Kondo peak. These features are associated to the noninteracting orbital structure of the molecular lobes (with some weight on Co orbital) rather than to levels fully localized at the Co atom. We have also been able to confirm the role of the surface density of states in defining the shape of the Fano dip suggested in Ref. 6. Our analysis illustrates the usefulness of simple models in systems where strong correlation effects preclude full *ab initio* studies.

ACKNOWLEDGMENTS

The authors are grateful to S.-W. Hla for a useful and encouraging correspondence. Financial support from the Spanish MCYT (Grants No. MAT2005-07369-C03-01 and No. NAN2004-09183-C10-08), the Universidad de Alicante, is acknowledged. G.C. is thankful to the Spanish "Ministerio de Educación y Ciencia" for a Ramón y Cajal grant. J.S. acknowledges the hospitality of the UA and partial financial support by the Conicet (Argentina). E.V.A. acknowledges the support of the Brazilian Agencies FAPERJ and CNPq.

[1] J. Kondo, Prog. Theor. Phys. **32**, 37 (1964).
[2] A. C. Hewson, *The Kondo Problem to Heavy Fermions* (Cambridge University Press, Cambridge, 1997).
[3] P. Wahl, L. Diekhoner, G. Wittich, L. Vitali, M. A. Schneider, and K. Kern, Phys. Rev. Lett. **95**, 166601 (2005).
[4] A. Zhao, Q. Li, L. Chen, H. Xiang, W. Wang, S. Pan, B. Wang, X. Xiao, J. Yang, J. G. Hou, and Q. Zhu, Science **309**, 1542 (2005).
[5] M. F. Crommie, Science **309**, 1501 (2005).
[6] V. Iancu, A. Deshpande, and S.-W. Hla, Nano Lett. **6**, 820 (2006).
[7] V. Iancu, A. Deshpande, and S.-W. Hla, Phys. Rev. Lett. **97**, 266603 (2006).
[8] L. Gao, W. Ji, Y. B. Hu, Z. H. Cheng, Z. T. Deng, Q. Liu, N. Jiang, X. Lin, W. Guo, S. X. Du, W. A. Hofer, X. C. Xie, and H.-J. Gao, Phys. Rev. Lett. **99**, 106402 (2007).
[9] U. Fano, Phys. Rev. **124**, 1866 (1961).
[10] G. Chiappe, E. Louis, E. SanFabián, and J. A. Verges, Phys. Rev. B **75**, 195104 (2007).
[11] G. Chiappe, E. Louis, E. V. Anda, and J. A. Vergés, Phys. Rev. B **71**, 241405(R) (2005).
[12] G. Chiappe and E. Louis, Phys. Rev. Lett. **97**, 076806 (2006).
[13] J. M. Aguiar-Hualde, G. Chiappe, E. Louis, and E. V. Anda, Phys. Rev. B **76**, 155427 (2007).
[14] J. A. Vergés and E. Louis, Solid State Commun. **22**, 663 (1977).
[15] P. W. Anderson, Phys. Rev. **124**, 41 (1961).
[16] J. Hubbard, Proc. R. Soc. London, Ser. A **276**, 238 (1963).
[17] A. Schiller and S. Hershfield, Phys. Rev. B **61**, 9036 (2000).
[18] G. Kotliar and A. E. Ruckenstein, Phys. Rev. Lett. **57**, 1362 (1986).
[19] Y. Meir, N. S. Wingreen, and P. A. Lee, Phys. Rev. Lett. **70**, 2601 (1993).
[20] J. M. Aguiar-Hualde, G. Chiappe, and E. V. Anda, Braz. J. Phys. **36**, 917 (2006).
[21] E. Vernek, N. Sandler, S. E. Ulloa, and E. V. Anda, Physica E **34**, 608 (2006).
[22] J. M. Aguiar-Hualde, G. Chiappe, and E. Louis, Phys. Rev. B **76**, 085314 (2007).
[23] E. V. Anda, G. Chiappe, C. A. Büsser, M. A. Davidovich, G. B. Martins, F. Heidrich-Meisner, and E. Dagotto, Phys. Rev. B **78**, 085308 (2008).
[24] Y. Meir and N. S. Wingreen, Phys. Rev. Lett. **68**, 2512 (1992).
[25] J. Merino and O. Gunnarsson, Phys. Rev. B **69**, 115404 (2004).
[26] O. Ujsaghy, J. Kroha, L. Szunyogh, and A. Zawadowski, Phys. Rev. Lett. **85**, 2557 (2000).
[27] V. M. Apel, M. A. Davidovich, G. Chiappe, and E. V. Anda, Phys. Rev. B **72**, 125302 (2005).
[28] Y. Tanaka and N. Kawakami, Phys. Rev. B **72**, 085304 (2005).
[29] K. Kang, S. Y. Cho, J.-J. Kim, and S. C. Shin, Phys. Rev. B **63**, 113304 (2001).
[30] B. R. Bulka and P. Stefanski, Phys. Rev. Lett. **86**, 5128 (2001).
[31] P. S. Cornaglia and C. A. Balseiro, Phys. Rev. B **67**, 205420 (2003).
[32] V. Madhavan, W. Chen, T. Jamneala, M. F. Crommie, and N. S. Wingreen, Science **280**, 567 (1998).
[33] N. Néel, J. Kröger, L. Limot, K. Palotas, W. A. Hofer, and R. Berndt, Phys. Rev. Lett. **98**, 016801 (2007).
[34] E. Louis, J. A. Vergés, J. J. Palacios, A. J. Pérez-Jiménez, and E. SanFabián, Phys. Rev. B **67**, 155321 (2003).
[35] D. A. Papaconstantopoulos, *Handbook of the Band Structure of Elemental Solids* (Plenum, New York, 1986).